Proceedings of the Eighteenth International Conference on
Civil, Structural and Environmental Engineering Computing
Edited by: P. Iványi, J. Kruis and B.H.V. Topping
Civil-Comp Conferences, Volume 10, Paper 3.8
Civil-Comp Press, Edinburgh, United Kingdom, 2025
ISSN: 2753-3239, doi: 10.4203/ccc.10.3.8


# Experimental Investigation on Lateral Vibration Control of a Small-Scale Three-Story Frame Using Locally Resonant Metamaterials

**Y. Choi, J. Choi and H. S. Park**

**Department of Architecture and Architectural Engineering,
Yonsei University,
Seoul, Republic of Korea**

## Abstract

This study experimentally investigates the effectiveness of locally resonant metamaterials (LRMs) in controlling lateral vibrations of a small-scale three-story steel frame. The LRMs were designed to target the structure's third natural mode, and acceleration responses were measured under varying numbers of LRM units. As the number of LRM units increased, the frequency distance between the side peaks (DP) widened, indicating an enhancement in bandgap-related behaviour. Modal Assurance Criterion (MAC) analysis revealed that the side peaks maintained strong similarity to the target mode shape. The performance of the LRMs was evaluated using two response reduction indicators, showing up to 95% attenuation near the local resonance frequency. While response reduction improved with more units, the effect was not strictly proportional, suggesting the need for future optimization in LRM design. These findings demonstrate the feasibility of applying LRMs to building structures for effective vibration control in low-frequency ranges.

**Keywords:** vibration control, locally resonant metamaterial, local resonant bandgap, modal characteristic, building structure, low-frequency vibration.

## 1 Introduction

Local resonant Metamaterials (LRMs) are a type of unit that controls vibration and noise by forming local resonance bandgaps (LRBGs) at specific frequencies. These LRBGs are formed by the resonant modes of local masses and effectively block wave propagation in the frequency range where the effective mass density becomes negative

[1, 2, 3]. Since its initial introduction by Liu et al. [4], LRM has been applied to various engineering cases. Most LRMs have been applied in high-frequency ranges above 100 Hz and have been primarily validated using small-scale experiments. In contrast, the frequency range of interest in civil and infrastructure engineering is typically below 100 Hz, and recent studies have reported the application of LRMs targeting this low-frequency domain.

Choi et al. [2] experimentally verified the formation of a bandgap around 40 Hz by applying a phononic crystal-type unit to a floating floor system in a residential building. In [5], a plate-type LRM was applied to a steel beam, while [1] and [6] investigated the use of sandwich-type LRMs on reinforced concrete slabs, both reporting vibration reduction effects near 40 Hz. These studies suggest the potential of LRMs as vibration control devices for structural members in the low-frequency domain commonly encountered in civil and infrastructure engineering.

Meanwhile, most LRMs have been applied to control flexural vibration of structural components, and there have been no reported cases of their application to the control of lateral vibration in building structures. In general, lateral vibrations are of interest in a much lower frequency range than flexural vibrations, particularly given that buildings typically exhibit relatively low natural frequencies. This necessitates the formation of bandgaps at frequencies significantly lower than those targeted by previously proposed LRMs. If these bandgaps can be effectively formed around a building's natural frequencies, the dynamic response within that range can be efficiently suppressed.

Therefore, this study experimentally investigates the lateral vibration control performance of a small-scale three-story steel frame attached with LRMs. The LRMs were specifically designed to target the third natural mode of the structure, and a series of experiments was performed with different numbers of LRMs to evaluate their effect. After attaching the LRM to the target structure, white noise excitation is applied using a shaking table, and the acceleration responses are measured. By comparing and analyzing the acceleration responses of the bare structure (without LRMs) and the LRM-attached structure, the study aims to demonstrate that LRM can be effectively applied to control lateral vibrations in the natural frequency range of the structure.

## 2 LRM unit Design

In general, the formation of the LRBG in a periodic array of LRMs is expressed by Equation (1) [2, 7, 8]:

$$LRBG = (f_r, f_r\sqrt{1+\mu}) \tag{1}$$

where $f_r$ is the local resonance frequency of the LRM unit, and $\mu$ is the mass ratio of the LRM to the host structure. This relationship has been both theoretically and experimentally shown to indicate the onset of LRBG at $f_r$.

In this study, the LRM unit was designed as shown in Figure 1(a), and the model can be represented as in Figure 1(b). The flexible beam of the LRM undergoes bending motion, while the head part, comprising most of the unit's mass, functions as a lumped mass. As a result, the LRM behaves as a mass–spring subsystem. By solving the eigenvalue problem in Equation (2) using the stiffness matrix K of the flexible beam and the mass matrix M of the head part, local resonance frequency $f_r$ can be determined, where $\omega$ represents the natural frequencies of the LRM unit.

$$det(K - \omega^2 M) = 0 \tag{2}$$

When the LRM units are periodically arranged, they respond to the horizontal motion of the host structure, as shown in Figure 1(c). This periodic arrangement enhances the LRBG behavior by effectively improving the wave attenuation performance within the LRBG [9]. Therefore, accurate estimation of $f_r$ and the LRBG is essential for the effective design of the LRM.

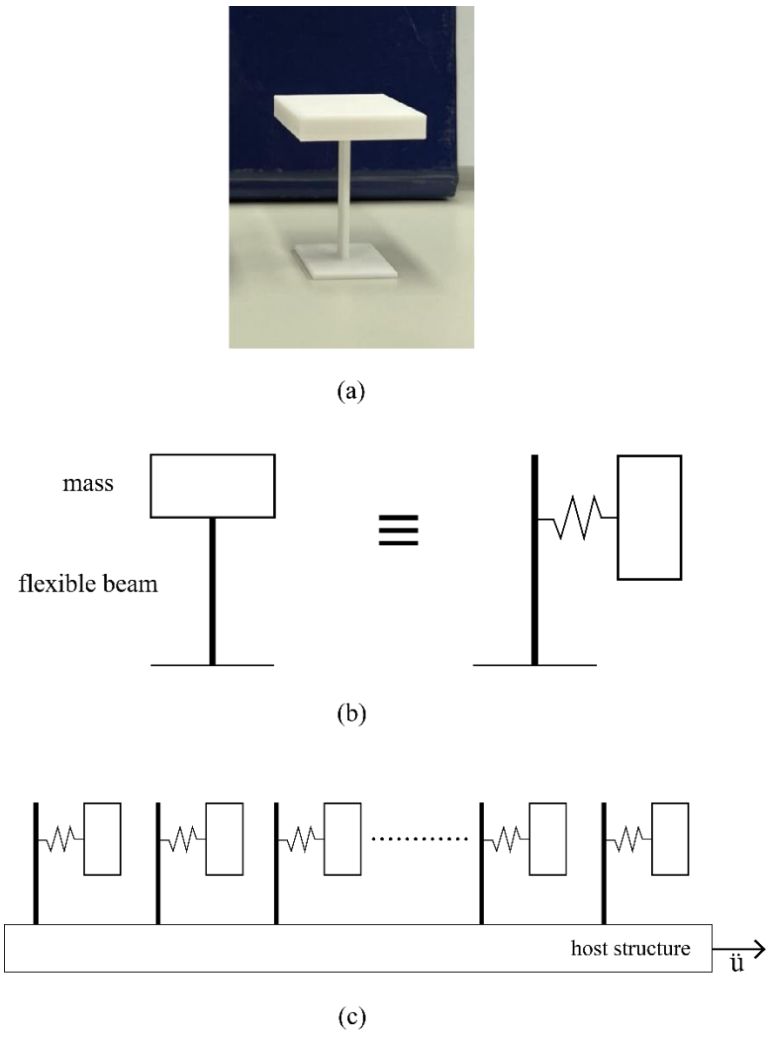


(a)

(b)

(c)

Figure 1: (a) LRM unit (b) Simplified model of LRM (c) Periodic arrangement of the LRM units.

## 3 Experimental setup

To investigate the lateral vibration control at the natural frequency of a building structure, LRMs were applied to a small-scale three-story steel frame. The host structure, as illustrated in Figure 2(a), is a 1.2 m tall single-bay steel frame, which was excited along its weak axis using a shaking table. White noise excitation with an RMS value of 0.15 g was applied for 180 seconds. Details of the host structure dimensions, LRM arrangement, sensor locations, and the overall experimental setup are illustrated in Figure 2(b). Accelerometers were installed on each floor, including the base, and the LRM units were attached to the third floor.

The first, second, and third natural frequencies of the host structure were identified as 6.3 Hz, 19.8 Hz, and 29.4 Hz, respectively. The LRMs were designed to target the third natural mode. The LRMs were fabricated using 3D printing, with polylactic acid (PLA) as the material. The density and Young's modulus of PLA are 1070 kg/m³ and 3000 MPa, respectively. The dimensions of the LRM head are $36\ \text{mm} \times 36\ \text{mm} \times 7\ \text{mm}$, and the flexible beam measures $2\ \text{mm} \times 6\ \text{mm} \times 44\ \text{mm}$. Unlike other vibration control techniques, LRMs locally resonate at the target frequency, so variations in vibration response are expected to occur primarily around the third mode frequency.

Acceleration responses were measured for three configurations: the bare structure (without LRMs), with 4 LRMs, and with 8 LRMs. The results were compared and analyzed to evaluate the effect of LRM attachment.

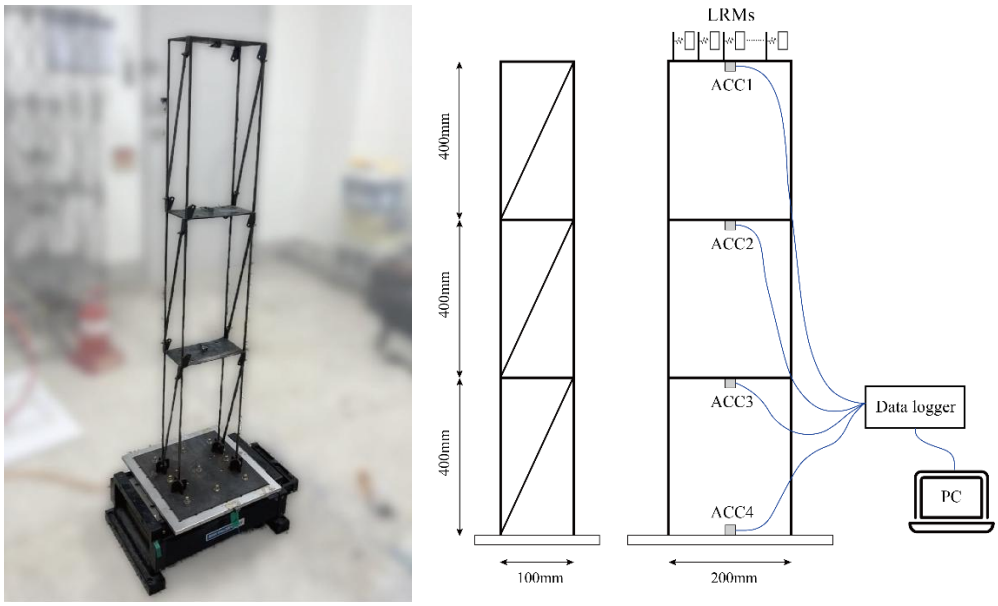


Figure 2: (a) Host structure (b) Details of experimental setup.

## 4 Results and Discussion

Figure 3 presents a comparison of the acceleration responses in the frequency domain at ACC1 for three configurations: the bare structure without LRMs, and the structure with 4 and 8 LRMs. The experimental results clearly show that the LRMs effectively reduce the acceleration response of the bare structure near the local resonance frequency range (29–33 Hz). Table 1 shows the mass ratios and the frequency distance between peaks (DP), which is used to evaluate the performance of the LRBGs, as proposed in [5]. Two distinct peaks appear around the local resonance frequency due to the LRMs, and it is observed that a higher mass ratio leads to a wider DP.

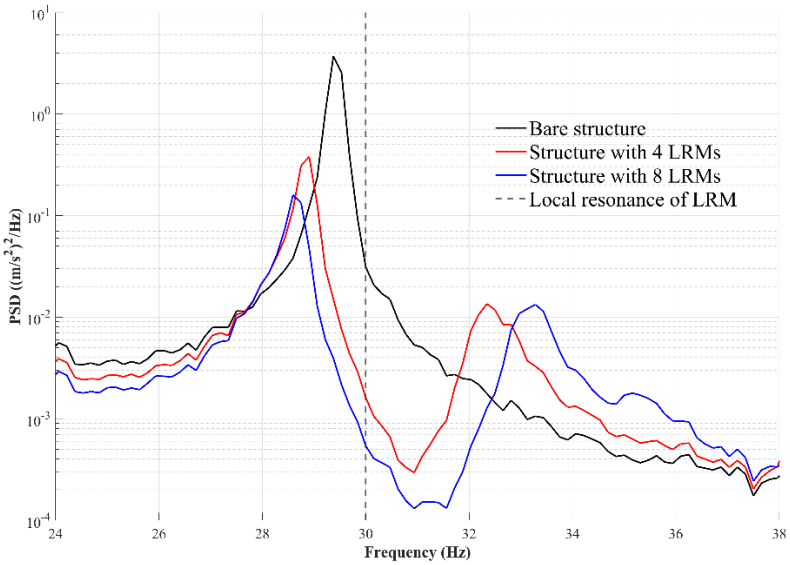


Figure 3: Acceleration response in the frequency domain at ACC1

| | Mass ratio | DP |
|---|---|---|
| 4 LRMs | 0.506 % | 2.4376 Hz |
| 8 LRMs | 1.012 % | 4.6874 Hz |

Table 1: Mass ratio and DP of each case.

Meanwhile, these side peaks are not generated by the bandgap behavior, but rather by the 2-DOF behavior of the system. When the LRBG—formed by the spring–mass subsystem of the LRM—is located close to a structural mode, the response is not uniformly attenuated. Instead, as reported in several studies [1, 5, 10, 11, 12], a pair of distinct peaks emerges on either side of the target frequency due to the coupled 2-DOF interaction between the structure and the resonators. To investigate the dynamic characteristics of these side peaks, the Modal Assurance Criterion (MAC), a widely used indicator for assessing the similarity between mode shapes, was employed. The MAC value is calculated using Equation (3), and the results—comparing each side peak with the third mode vector of the bare structure—are presented in Table 2.

$$MAC = \frac{|\{\Psi_i\}^T\{\Psi_j\}|^2}{(\{\Psi_i\}^T\{\Psi_i\})\left(\{\Psi_j\}^T\{\Psi_j\}\right)} \quad (3)$$

In both cases, the left peak exhibits a MAC value close to 1, indicating that the mode vector is nearly identical to the target mode shape of the bare structure. In contrast, the MAC values for the right peak are relatively lower in both cases. This is considered to result from the fact that the local resonance frequency of the LRM used in this study is slightly higher than the target mode frequency, causing the right peak to deviate further from the target mode compared to the left peak. However, as shown in Figure 4, the mode shape of the right peak still exhibits a similar pattern to the third mode shape of the bare structure.

| | Left peak & target mode | Right peak & target mode |
|---|---|---|
| 4 LRMs | 0.985 | 0.769 |
| 8 LRMs | 0.963 | 0.697 |

Table 2: MAC comparison between side peaks and target mode shape.

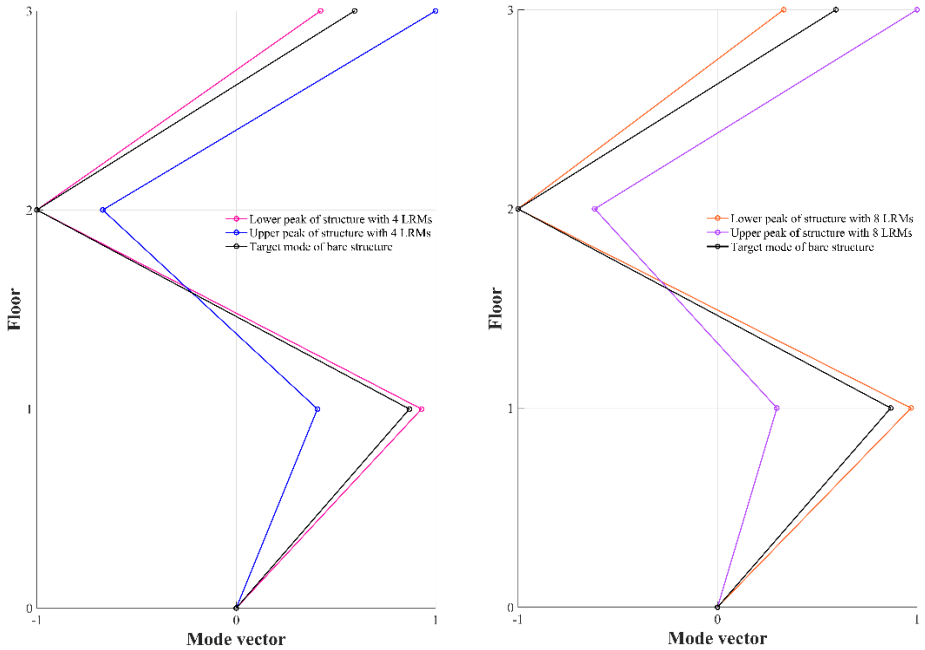


Figure 4: Comparison of mode shapes at side peaks with the target mode shape of the bare structure (a) 4 LRMs (b) 8 LRMs

Meanwhile, quantitatively evaluating the structural response is an important indicator for assessing both the safety and serviceability of a structure. Accordingly, the response reduction performance achieved by the LRMs was evaluated using Equation (4) and Equation (5), as proposed by Choi et al. [5].

$$RSiR = (P_b - P_c)/P_b \times 100(\%) \quad (4)$$

$$PRSR = (P_p - \max(P_l, P_u))/P_p \times 100(\%) \quad (5)$$

The response suppression ratio in local resonance frequency (RSiR) evaluates the reduction in response at the target local resonance frequency and the peak response suppression ratio (PRSR) assesses the maximum response reduction. Here, $P_b$ and $P_c$ represent the responses of the bare structure without LRMs and the structure with LRMs, respectively, at the LRM's resonance frequency. $P_p$ denotes the maximum response of the bare structure, and $P_l$ and $P_u$ indicate the responses at the lower and upper peaks of the structure with LRMs, respectively. Tables 3 and Table 4 present the RSiR and PRSR values at each measurement location for different numbers of LRMs. In both RSiR and PRSR, the response reduction performance improved with increasing mass ratio and higher measurement location. In all cases, the response reduction rate exceeded 70%, indicating a high response reduction performance. Notably, when 8 LRMs were applied, both indices exhibited reduction rates over 95% at ACC1, confirming the effectiveness of the LRM in suppressing the structural response. However, the results show that the response reduction performance does not increase proportionally with the number of LRMs, suggesting that it is necessary to evaluate the optimal performance of the LRM design using systematic algorithms in the future.

| | ACC1 | ACC2 | ACC3 |
|---|---|---|---|
| 4 LRMs | 94.81 % | 80.55 % | 69.59 % |
| 8 LRMs | 98.26 % | 86.35 % | 75.18 % |

Table 3: RSiR values at each measurement location.

| | ACC1 | ACC2 | ACC3 |
|---|---|---|---|
| 4 LRMs | 89.76 % | 76.91 % | 72.14 % |
| 8 LRMs | 95.68 % | 84.14 % | 79.48 % |

Table 4: PRSR value at each measurement location.

## 5 Conclusions and Contributions

In this study, the lateral vibration control performance of a small-scale three-story steel frame was experimentally investigated through the application of LRMs. The LRMs were specifically designed to target the host structure's third natural mode, and experiments were conducted under various LRM configurations while measuring acceleration responses on each floor.

The experimental results demonstrate that the LRMs significantly reduced the acceleration response of the host structure within the local resonance frequency range (29–33 Hz). In addition, increasing the number of LRMs led to a widening of DP. To assess the modal similarity between the side peaks and the target frequency, MAC

was calculated. The left side peak exhibited a MAC value close to 1, indicating an almost identical mode shape to the target mode, whereas the right side peak, though slightly different, still exhibited similar modal characteristics. Although both RSiR and PRSR improved with the addition of LRMs, the increase in response reduction performance was not proportional to the number of units applied. This finding suggests that future studies should explore the optimal performance of LRM design through systematic optimization approaches.

In summary, the results confirm that properly designed LRMs can effectively suppress lateral vibrations near a structure's natural frequencies. In particular, the study demonstrates the potential for applying LRMs in building structures where vibration control below 100 Hz is critical—a key distinction from conventional metamaterial research focused on high frequencies.

## Acknowledgements

This work was supported by the National Research Foundation of Korea (NRF) grant funded by the Korea government Ministry of Science (No. 2021R1A2C3008989).

# References

[1] J. Choi, T. Hong, D.E. Lee, T. Cho, H.S. Park, "Hybrid behaviors of RC metaslab combining bandgap and isolation for broadband vibration control", *International Journal of Mechanical Sciences*, 267, 109004, 2024, DOI:10.1016/j.ijmecsci.2024.109004.

[2] J. Choi, T. Cho, S.G. Bae, H.S. Park, "Development and practical application of locally resonant metamaterials for attenuation of noise and flexural vibration of floors in residential buildings", *Journal of Building Engineering*, 57, 104907, 2022, DOI:10.1016/j.jobe.2022.104907.

[3] Z. Liu, C.T. Chan, P. Sheng, "Analytic model of phononic crystals with local resonances", *Physical Review B: Condensed Matter and Materials Physics*, 71(1), 014103, 2005, DOI:10.1103/PhysRevB.71.014103.

[4] Z. Liu, X. Zhang, Y. Mao, Y.Y. Zhu, Z. Yang, C.T. Chan, P. Sheng, "Locally resonant sonic materials", *Science*, 289(5485), 1734–1736, 2000, DOI:10.1126/science.289.5485.1734.

[5] J. Choi, T. Cho, H.S. Park, "Design and performance evaluation of steel beam members with plate-type locally resonant metamaterials for vibration control", *Computer-Aided Civil and Infrastructure Engineering*, 38(12), 1622–1637, 2023, DOI:10.1111/mice.12926.

[6] J. Choi, B.W. In, T. Hong, D.E. Lee, T. Cho, H.S. Park, "Low-frequency vibration and noise control in sandwiched composite locally resonant metamaterials-embedded plate structures", *Developments in the Built Environment*, 18, 100457, 2024, DOI:10.1016/j.dibe.2024.100457.

[7] C. Sugino, Y. Xia, S. Leadenham, M. Ruzzene, A. Erturk, "A general theory for bandgap estimation in locally resonant metastructures", *Journal of Sound and Vibration*, 406, 104–123, 2017, DOI:10.1016/j.jsv.2017.06.004.

[8] C. Sugino, S. Leadenham, M. Ruzzene, A. Erturk, "On the mechanism of bandgap formation in locally resonant finite elastic metamaterials", *Journal of Applied Physics*, 120(13), 134501, 2016, DOI:10.1063/1.4963648.

[9] P. Guo, Q. Zhou, J. Yang, X. He, Z. Luo, "The low-frequency vibration control mechanism of a finite locally resonant beam with elastic supports", *Journal of Vibration Engineering & Technologies*, 12, 3919–3930, 2023, DOI:10.1007/s42417-023-01096-z.

[10] V.C. De Sousa, D. Tan, C. De Marqui, A. Erturk, "Tunable metamaterial beam with shape memory alloy resonators: Theory and experiment", *Applied Physics Letters*, 113(14), 143502, 2018, DOI:10.1063/1.5050213.

[11] J.S. Chen, B. Sharma, C.T. Sun, "Dynamic behaviour of sandwich structure containing spring mass resonators", *Composite Structures*, 93(8), 2120–2125, 2011, DOI:10.1016/j.compstruct.2011.02.007.

[12] H. Peng, P.F. Pai, "Acoustic metamaterial plates for elastic wave absorption and structural vibration suppression", *International Journal of Mechanical Sciences*, 89, 350–361, 2014, DOI:10.1016/j.ijmecsci.2014.09.018.